Journal of Orthopaedic Research
12:375-383 The Journal of Bone and Joint Surgery, Inc.

Mathematical Model for the Mineralization of Bone

Bruce Martin

Orthopaedic Research Laboratories, University of California, Davis, Sacramento, California, U.S.A.

Summary: A mathematical model is presented for the transport and precipitation of mineral in refilling osteons. One goal of this model was to explain calcification "halos," in which the bone near the haversian canal is more highly mineralized than the more peripheral lamellae, which have been mineralizing longer. It was assumed that the precipitation rate of mineral is proportional to the difference between the local concentration of calcium ions and an equilibrium concentration and that the transport of ions is by either diffusion or some other concentration gradient-dependent process. Transport of ions was assumed to be slowed by the accumulation of mineral in the matrix along the transport path. The model also mimics bone apposition, slowing of apposition during refilling, and mineralization lag time. It was found that simple diffusion cannot account for the transport of calcium ions into mineralizing bone, because the diffusion coefficient is two orders of magnitude too low. If a more rapid concentration gradient-driven means of transport exists, the model demonstrates that osteonal geometry and variable rate of refilling work together to produce calcification halos, as well as the primary and secondary calcification effect reported in the literature.

In the last 50 years, the mineralization of bone has received much attention. Historically, many investigators have focused on the difficulty in the initiation of calcification caused by the metastability of interstitial fluid with respect to hydroxyapatite. Others have directed their attention to the structure of the completed mineral-organic complex. A foundation of basic concepts concerning the initial calcification processes and mineral-collagen structures has been built (2).

Events occurring between the initiation of calcification and the completion of the fully calcified structure have received less attention. So-called primary calcification takes only a few days, but the final 30% or so of the mineral takes months to put in place (1,9,16). Little is known about the means by which calcium is transported from the bone surface through layers of partially mineralized matrix to complete calcification of the still deeper lamellae. Diffusion is at least implicitly assumed to play a role (13), but it also is widely thought that cells actively transport ions during mineralization (16,19).

Also, earlier concepts of calcium homeostasis recently have begun to give way to theories based on the exchange of bone mineral exclusive of remodeling (15). These theories cannot be fully elaborated until the transport, precipitation, and equilibrium of bone mineral are understood more completely.

Observation of osteonal bone may provide insights regarding the transport of mineral during completion of calcification. Microradiographs illustrate not only variations in mineral distribution between old and new osteons but also patterns of distribution within the osteonal wall. Figure 1 shows that the innermost osteonal lamellae of newly formed osteons commonly are more radiopaque than lamellae farther out, which were laid down earlier and have been mineralizing longer. Something about the transport and precipitation of mineral tends to produce a calcification "halo" adjacent to the canal

Received December 15, 1992; accepted July 2, 1993.
Address correspondence and reprint requests to Dr. R. B. Martin at Orthopaedic Research Laboratories, University of California Davis Medical Center Research Facility, Room 2000, 4815 Second Avenue, Sacramento, CA 95817, U.S.A.

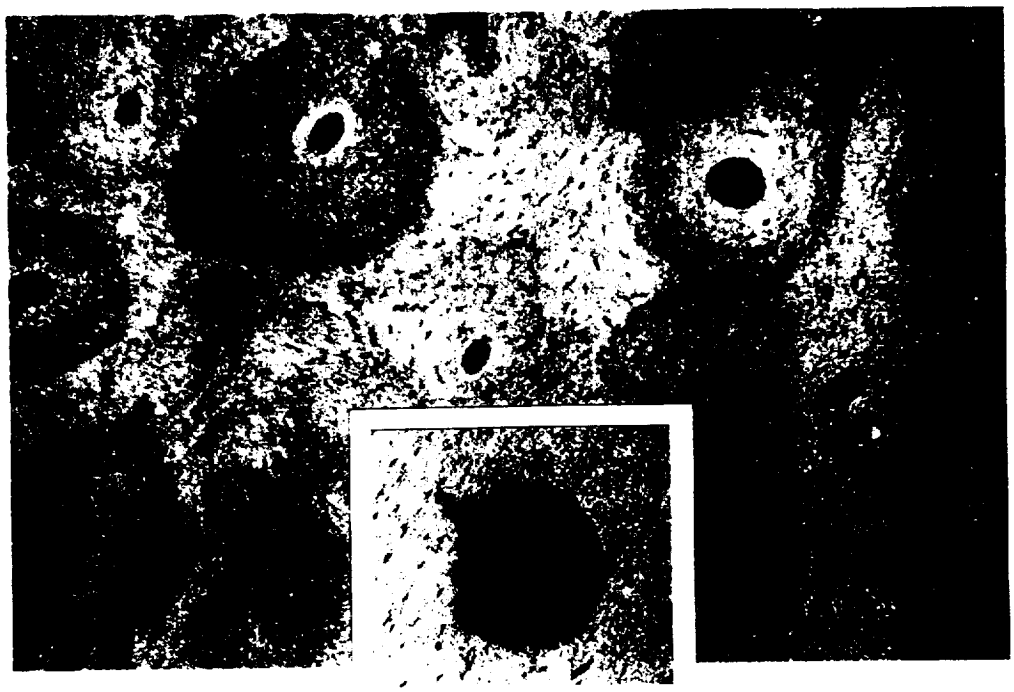

FIG. 1. Microradiograph of osteonal bone from rhesus monkey, showing variability in mineralization among osteons and the common occurrence of a "halo" of more heavily mineralized bone near the canal surface. The approximate field width is 1,000 μm. Inset: Osteons just beginning to refill lack such a halo.

(Fig. 2). Mineral density is high near the haversian canal, low in the middle lamellae, and increases again near the cement line. Weaver (22) established that the hardness of bone correlates with the halo; it is elevated near the haversian canal.

I present here a mathematical model for the transport and precipitation of mineral in osteons; the model is intended to be a tool for achieving a better understanding of the middle ground between the initiation of calcification and the completion of the calcified matrix. It addresses the following questions: (a) Can classic diffusion and precipitation equations serve as the basis for a finite-element model that converges on stable solutions and completes calcification in the observed period of time? (b) Does such a model produce calcification halos? (c) Does such a model exhibit primary and secondary mineralization behavior? (d) How is osteonal calcification affected by the geometry and dynamics of osteonal refilling, as opposed to crystal formation *per se*?

METHODS

Assumptions

The present model does not deal directly with the complex and still unresolved issues surrounding the nucleation and growth of bone mineral crystals; it is concerned with the accumulation of mineral in the bone matrix once nucleation has occurred. Mineralization may involve the precipitation of a sequence of calcium phosphates having different solubilities (5,12). However, for the sake of the construction of an initial model, it was assumed that a single mineral (hydroxyapatite) is formed and that its rate of pre-

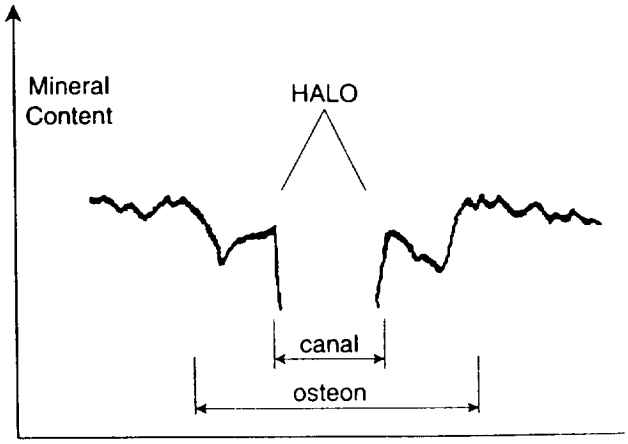

FIG. 2. Graph showing the result of scanning across the microradiographic image of a mineralizing osteon. Radiographic density is plotted against scan position. The central depression is the haversian canal. There is a relatively high mineral content near the wall of the haversian canal and near the cement line. The interior of the wall is less mineralized. Modified from Amprino and Engström (1).

cipitation is proportional to the difference between the local concentration of a single ion (calcium) and its equilibrium concentration (15).

The model assumes that transport of ions is by either diffusion or another concentration gradient-driven mechanism. For example, transport of calcium ions via the osteocyte-canalicular network could be driven by the difference in the concentration of this ion across the network. Thus, in what follows, the word diffusion should not be interpreted literally; indeed, the analysis will demonstrate that simple diffusion cannot be the primary transport mechanism.

With this said, the model is based on Fick's Laws for diffusion, and it was assumed that transport of ions is controlled by the concentration gradient across, and the "diffusion" coefficient within, the matrix through which the ions must pass. The governing equation is written in two-dimensional form so that curved osteonal bone-forming surfaces can be treated:

$$\frac{\partial C}{\partial t} = \frac{\partial}{\partial x}\left(D \frac{\partial C}{\partial x}\right) + \frac{\partial}{\partial y}\left(D \frac{\partial C}{\partial y}\right) - P \qquad (1)$$

Here, C is the concentration of a specific ion species; D is an isotropic diffusion (or transport) coefficient for this ion; x and y are directions normal and parallel to the mineralizing surface, respectively; t is time; and P is the rate of precipitation of mineral ions from solution. For the sake of simplicity, it is assumed that Eq. 1 describes the transport and precipitation of calcium ions alone.

The concentration is given as milligrams of free calcium per milliliter of interstitial fluid, and the rate of precipitation is given as milligrams of calcium precipitated per milliliter of interstitial fluid per second. To simplify matters, the rate of precipitation includes the nucleation of new crystals and growth of existing crystals. The rate is assumed to be proportional to the difference between the local concentration of calcium ions (C) and an equilibrium concentration (C_{eq}):

$$P = k_{cal}\,(C - C_{eq})^n \qquad (2)$$

where k_{cal} is a rate coefficient and n is a small number (12,15). This relationship is not limited to precipitation; it is assumed that if $C < C_{eq}$, mineral crystals will dissolve.

Calcification (Γ) is defined as milligrams of calcium in hydroxyapatite per milliliter of bone. Typically, 1 ml of cortical bone contains about 2 g of calcified matrix, of which 1.26 g is mineral, primarily hydroxyapatite (23). Since, by weight, 40% of hydroxyapatite is calcium, the average calcium content of cortical bone, Γ^*, is approximately 500 mg/ml.

Microporosity is defined as the water-filled space amidst the collagen molecules and mineral crystals in the calcified matrix. The microporosity of osteoid contains the space to be filled by mineral, as well as the water that is bound to collagen or mineral, or both, and cannot be displaced. The volume fraction of the micropores is denoted by V_w.

The diffusion and precipitation of ions depend on the concentration of ions in the interstitial fluid within the micropores of the mineralizing matrix. Therefore, ionic concentration needs to be expressed per unit volume of interstitial fluid, not per unit volume of bone. On the other hand, the rate of accumulation of crystalline mineral per cubic millimeter of bone clearly depends on the volume fraction of the micropores; if this volume fraction is small, there will be less interstitial fluid from which mineral ions can be precipitated into crystals, and the rate of calcification will be small relative to the rate of precipitation. Thus, the rate of accumulation of crystalline calcium, $d\Gamma/dt$, is assumed to be

$$d\Gamma/dt = PV_w \qquad (3)$$

It is assumed that the volume fraction of mineral is zero in osteoid and that the organic fraction is the same in osteoid as in fully mineralized bone. As osteoid mineralizes, mineral displaces interstitial fluid, reducing its volume fraction from about 66% to about 28% (23). This greatly diminishes the solute space through which mineral ions diffuse to reach growing hydroxyapatite crystals. The diffusion coefficient is assumed to diminish as mineral accumulates in the matrix, slowing transport. Neuman (13) hypothesized this phenomenon as follows. "As the crystals grow, they must grow closer and closer together, the hydration shells must ultimately interact, and the diffusion of ions through the highly concentrated jackets. . . becomes slower and slower. As the crystal faces approach each another, the restriction of charge and volume gradually will slow diffusion to a point where it is stopped almost completely."

Thus, as calcification increases, it is assumed that the diffusion coefficient (D) decreases. A diffusion-calcification coefficient, k_{dc}, is postulated such that

$$D = D_0 \exp(-k_{dc}\Gamma) \qquad (4)$$

where D_0 is the diffusion coefficient for osteoid.

Finally, the model incorporates two observations about osteonal refilling. First, as an osteon refills, the

area of the bone-forming surface (through which ions must pass to reach deeper lamellae) grows steadily smaller, "choking" the supply of mineral. Also, the innermost lamellae are laid down more slowly than the outer lamellae (8,10), giving them more time in close proximity to the source of ions.

Model

The model is based on the simultaneous application of the equations to an idealized bone-forming site (Fig. 3). Bone is being laid down by osteoblasts,

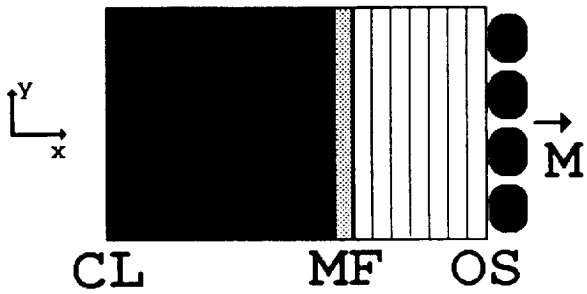

FIG. 3. Schematic diagram showing a developing wall of new bone. Osteoblasts (dark ovals) are advancing the osteoid surface (OS) in the x direction with velocity M. Behind the osteoid (white region), a mineralization front (MF) follows at the same velocity. Bone formation began on a cement line (CL). The evenly spaced vertical lines show the relative x dimension of the elements used in the finite-element mesh. The completed osteonal wall contained 60 such elements.

starting on a cement line. The bone behind the cement line is assumed to be fully mineralized, but its mineral cannot move into the region of new bone. This is justified by the observation that, on microradiographs (Fig. 1), a sharp line of demarcation is seen at the cement line when a partially calcified new osteon lies within a region of fully calcified bone. There is no evidence that mineral "leaches out" of the old matrix and crosses the cement line (1).

The apposition rate of osteoid (M, in μm/day) is in the x direction. The surface of the osteoid in contact with the osteoblasts is termed the osteoid surface. At the mineralization lag time (T_{lag}, in days), after a layer of osteoid has been laid down, it begins to mineralize, forming a mineralization surface. The mineralization surface subsequently follows the osteoblasts away from the cement line, moving to the right with velocity M. When bone formation ceases, the distance between the cement line and the osteoid surface is the wall thickness (X_{wall}) of the completed formation site.

Taken together, these equations constitute a nonlinear system for which a closed-form solution would be very difficult. Therefore, a computer program in compiled BASIC (BV10-5) by Bear and Verruijt (3) was modified to solve Eq. 1 while satisfying the other equations as well. Their program uses a central finite-difference method to determine the transient behavior of a finite-element model for Eq. 1. They have described the details of the finite-element solution and verification of its convergence to a closed-form solution (3). Their program was modified to simulate the continuous apposition of osteoid and other assumptions as follows.

A mesh containing N elements, each $X_{elem} = X_{wall}/N$ mm thick (x dimension), is defined (Fig. 4). To simulate refilling of a segment of an osteon, a wedge-shaped mesh is created by letting the y dimension of each element linearly diminish so that the heights of the first and last elements are in proportion to the ratio of the radius of the cement line to the radius of the haversian canal. For other testing, a rectangular mesh is used.

The mesh defines a completed wall of new bone. Initially, however, the model consists of only the leftmost element, with its right edge nodes fixed at C_0 to represent the presence of a vascular supply of

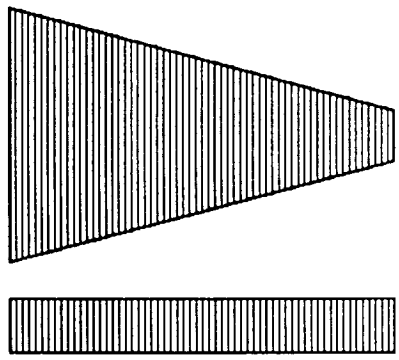

FIG. 4. Drawn-to-scale illustrations of the meshes used in the finite-element model. The top, wedge-shaped mesh containing 60 elements, was used for the osteonal model. Each element is 1.333 μm wide. The heights of the first (farthest left) and last elements are 50 and 10 μm, respectively. The lower mesh, representing formation on a flat surface, was the 60 element model used in the convergence test. Its overall dimensions were 80 × 10 μm. Other meshes used in the test were of the same overall width and height but contained 30, 40, 50, and 70 elements of uniform width.

calcium ions at the osteoid surface. Its left edge nodes are initially set equal to C_0, but allowed to vary, and its diffusion coefficient is set equal to D_0. This starting model is solved incrementally over the time required to lay down a single element (X_{elem}/M). At the end of each time increment (δt), the rate of precipitation (P) within the element is calculated

TABLE 1. *Baseline values of model variables*

D_0 = 0.10 mm²/sec	Diffusion coefficient for osteoid
K_{dc} = 0.001 ml/mg	Diffusion-calcification coefficient
C_0 = 0.05 mg/ml	Calcium concentration at free surface
C_{eq} = 0.01 mg/ml	Equilibrium calcium concentration
K_{cal} = 2.0 mm³/mg-sec	Crystal growth rate coefficient
n = 2	Crystal growth rate exponent
Γ^* = 500 mg/ml	Calcification of fully mineralized bone
d_{min} = 3,300 mg/ml	Density of bone mineral
V_{org} = 0.34	Volume fraction of organic phase
T_{lag} = 10 days	Mineralization lag time
K_{fill} = 0.02 day⁻¹	Nonlinear refilling coefficient

from the mean of the element's nodal concentrations by Eq. 2. The calcification of the element is calculated as

$$\Gamma = \Gamma' + PV_w\delta t \qquad (5)$$

where Γ' is the calcification at the end of the previous time period, $PV_w\delta t$ is the amount of calcium precipitated per milliliter of bone during the current time increment, and $V_w = 1 - V_{org} - V_{min}$. Here, V_{org} is the volume fraction of the organic part of the bone, taken to be constant at 0.34 (23). V_{min} is the mineral volume fraction, taken to be $\Gamma/(m_{ca}\, d_{min})$, where m_{ca} = 0.40 mg of calcium per milligram of hydroxyapatite and d_{min} = 3,300 mg/ml, or the specific gravity of hydroxyapatite (21). Then, the diffusion coefficient of the element is calculated from the calcification (Γ) by Eq. 4, and the model is solved again for the next time increment.

When it is time to add another element to the model (X_{elem}/M = about 1 day), the mesh is redefined to include a second element; the right nodes of the new element are fixed at C_0, and the left nodes (which had been the fixed right nodes of the original element) are made variable. The original element continues with the same initial values for the concentration at its nodes and for the diffusion coefficient and calcification (Γ) that it had at the end of the previous time period. (This is a mixed initial-value/boundary-value problem.) The new element is assigned $D = D_0$ and $\Gamma = 0$. This revised model then is solved through another X_{elem}/M time interval. By continuation of this process, all N elements are added to the model. After the last element has been added, the model is run an additional 200 days to approximate the completion of mineralization.

To account for the mineralization lag time, elements are not allowed to begin precipitating calcium until they have been in the model for T_{lag} days, creating an osteoid seam, where $k_{cal} = P = \Gamma = 0$ and $D = D_0$. Precipitation was halted when $\Gamma = \Gamma^*$, defined as complete mineralization.

The rate of apposition decreases during osteonal refilling (8,11) according to

$$M = dR/dt = k_{fill}R \qquad (6)$$

where k_{fill} is a refilling rate coefficient. To model this effect, R is assumed to be equal to the radius of the cement line minus the thickness of the wall added thus far, and the rate of apposition is recalculated for each new element.

To determine an appropriate element size, a series of rectangular (Fig. 4), constant rate of apposition models of increasing resolution was tested with use of the model's parameters (Table 1). Figure 5 shows the results of this convergence test. The effect of element size rapidly diminishes as N approaches 70 elements. To restrict the solution time to about 1 hour (on a 486 personal computer operated at 33 MHz), N = 60 was chosen for the analyses reported here.

The speed and accuracy of the model also are affected by δt. For accuracy, when a new element is

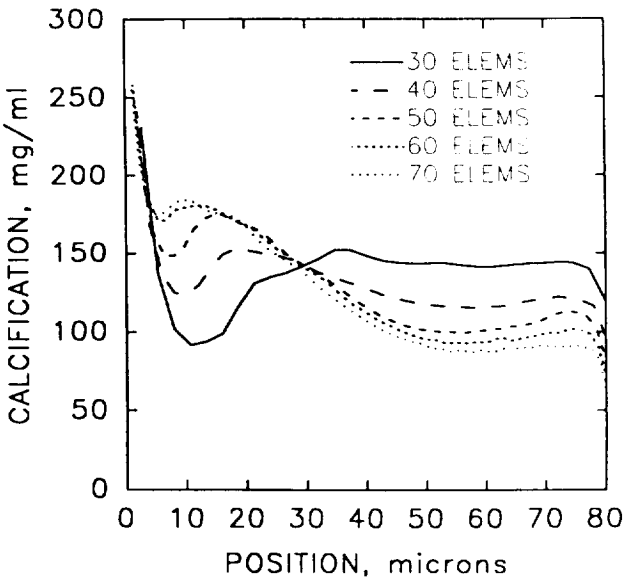

FIG. 5. Calcification plotted against position in the wall of newly formed bone for five models containing increasing numbers of elements. This test of the effect of element size and number on the behavior of the model used a model configured for bone formation on a flat surface with a constant apposition rate (k_{cal} = 1.0 mm³/mg-sec) and a mineralization lag time of 0 days.

added, the first δt should be $\leq (X_{elem})^2/2D_0 \approx 10^{-5}$ sec (3). Fortunately, δt need not remain this small because the rate of change within the model diminishes with time (3). Therefore, δt is increased gradually, with the sequence (in seconds) of 0.00001, 0.00003, 0.0001, 0.0003, 0.001, 0.003, and so on. Testing showed that this did not affect the results significantly.

Selection of Parametric Values

Values to be used for the variables in the model must be estimated. For lack of data, these baseline values often were chosen rather arbitrarily, but in each case they were tested by varying them parametrically in the model until each gave results consistent with observed temporal and spatial patterns of mineralization.

The baseline values for the mineralization lag time (10 days), radius of the cement line (R_O, 0.100 mm), radius of the haversian canal (R_h, 0.020 mm), refilling time (T_{fill}, 80 days), and completed wall thickness ($R_c - R_h$, 0.080 mm) are typical of values in the literature (11). The refilling coefficient was calculated from Eq. 6 as $k_{fill} = -\ln(R_h/R_O)/T_{fill} = 0.020$ day^{-1}, with use of the baseline values. The equivalent mean rate of apposition was 0.001 mm/day. For convenience, complete calcification (Γ^*), was set equal to the average calcification (500 mg/ml) calculated earlier for cortical bone.

The concentration of calcium in blood serum is about 2.48 m*M* or 0.10 mg/ml (7). Of this calcium, about 48% is free (not bound to proteins). The concentration of calcium ions in interstitial fluid is thought to be somewhat more than half of that in blood plasma (20), but a higher proportion is free. Therefore, a reasonable estimate of the concentration of calcium at the osteoid surface is 0.05 mg/ml.

No data were found for the diffusion of calcium or phosphate ions through collagenous tissue or bone. The measurement of the diffusion of these ions through bone is confounded by the fact that when a concentration gradient is placed across the tissue, these ions are apt to precipitate within, or dissolve out of, the bone, as well as diffuse through it (14). Therefore, it is necessary to estimate the diffusion coefficient indirectly.

The diffusion coefficient for strong electrolyte ions (such as calcium) in water at room temperature is slightly larger than 1×10^{-5} cm^2/sec (21). Boskey (6) determined the diffusion coefficient for calcium ions in denatured collagen gels to be $6.0 \pm 0.5 \times 10^{-6}$ cm^2/sec. On the basis of these limited observations, a reasonable baseline value for the diffusion coefficient of calcium ions through osteoid (D_0) would be 5×10^{-6} cm^2/sec = 0.0005 mm^2/sec. However, when this value was tried in the model, it was found to be much too low to produce observed levels of calcification. After testing of various values, D_0 = 0.10 mm^2/sec was selected as a baseline value. Also, lacking experimental data, 0.001 ml/mg was assigned as a baseline value for the diffusion-calcification coefficient (k_{dc}) after testing of various values in the model.

To learn how well Eq. 3 applies to the precipitation of hydroxyapatite, an experiment by Boskey and Posner (4), and reported on by Wuthier (24), was analyzed. In this experiment, hydroxyapatite crystals were grown in a solution without replenishment of the calcium (or phosphate) ions. An equation describing this situation was derived with use of Eq. 3 and found to fit the experimental data very well when n = 2. The result also showed that the equilibrium concentration (C_{eq}) was 0.025 mg/ml if the precipitating "seed" was a phospholipid, and 0.006 mg/ml if it was hydroxyapatite crystals. Corresponding values of the rate coefficient (k_{cal}) were assumed inappropriate for the model because nucleation sites were probably much more sparse in the experiment. After different values of the rate coefficient and the equilibrium concentration were tried in the model, baseline values of 2.0 ml/mg-sec and 0.01 mg/ml, respectively, were selected.

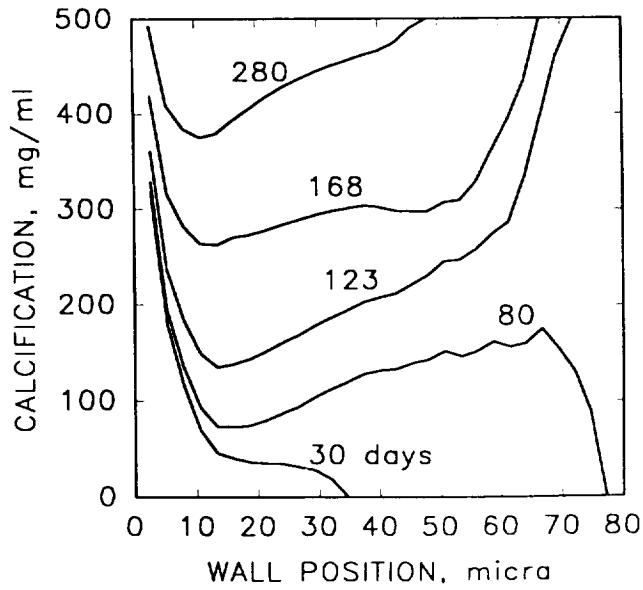

FIG. 6. Calcification profiles (Γ compared with position in the osteonal wall) are shown 30, 80, 123, 168, and 280 days after the start of refilling at a variable rate with baseline parametric values.

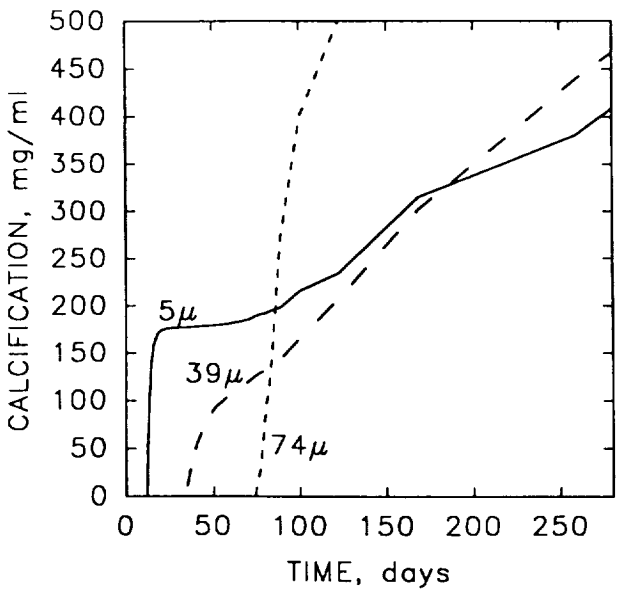

FIG. 7. Graph showing temporal changes in calcification at three representative locations in an osteonal wall: near the cement line (5 μm), in the middle (39 μm), and near the haversian canal (74 μm). The first two curves exhibit primary (steep slope) followed by secondary (reduced slope) mineralization behavior.

RESULTS

Extensive testing of the model showed that when its parameters were kept within the vicinity of the baseline values, it was stable and insensitive to refinements of element size and time increments. However, as previously mentioned, the model does not support the concept of transport by simple diffusion because, no matter how much time is allowed or how other parameters are adjusted, the values for diffusion of calcium ions in collagen gels did not produce physiological levels of calcification. As 0.03 mm^2/sec was exceeded, the model began to approximate physiologic results, and values in the vicinity of the baseline of 0.10 mm^2/sec produced nearly complete calcification at 280 days.

Early in the refilling process (30 days), there was no indication of a calcification halo (Fig. 6). This concurs with the appearance of the osteon beginning to refill in Fig. 1. Before refilling ended, however, a halo emerged, and in the newly completed osteon (80 days), the profile was quite similar to that in Fig. 2. There was a peak of calcification near the canal surface, a valley in the central region of the wall, and a return to high levels near the cement line. As calcification continued after the cessation of bone formation, the region nearest the canal surface continued to mineralize faster than deeper regions (145 days), and a state of "complete mineralization" slowly worked its way toward the cement line.

The model also exhibited primary and secondary calcification (Fig. 7). In the lamellae near the cement line and in the middle of the wall, there was an initial rapid calcification followed by a much slower rate of mineral accumulation. This profile is similar to that of primary and secondary calcification as described by Parfitt (16). However, the model predicted that lamellae laid down near the end of osteonal refilling rapidly reach full calcification.

The comparison of the behavior of "flat" and osteonal models (data not shown), with and without variable rates of apposition, showed that calcification halos are caused primarily by the variable refilling rate and secondarily by the bottle-neck effect. Also, experimentation with the model showed that achievement of physiologic calcification levels depends on parameters being within a fairly narrow range. For example, varying the diffusion-calcification coefficient (k_{dc}) had little effect while the osteon was refilling, but values less or greater than the baseline value retarded completion of mineralization; increasing the rate coefficient (k_{cal}) over the baseline value enhanced calcification during refilling but later resulted in reduced mid-wall calcification.

DISCUSSION

The goal of this work was to answer several questions concerning a mathematical model of mineralization based on classic equations for diffusion and precipitation. Does such a model exhibit stable and convergent behavior and produce observed levels of calcification in physiologic periods of time? The answer to the first part of this question is yes. The answer to the second part also is yes, but only if the rate of ion transport is much greater than that provided by simple diffusion. Does the model produce calcification halos and exhibit primary and secondary mineralization rates? The answers to both these questions are definitely yes. Finally, is osteonal mineralization affected by osteonal geometry and refilling dynamics? Indeed, these factors were found to be primarily responsible for halo formation.

Schmidt, in 1933, as cited by Amprino and Engström (1), attributed the greater degree of calcification of the inner osteonal lamellae to their slower rate of apposition, but the latter authors believed that this was immaterial; they postulated that the inner lamellae were more calcified because they were closer to the vascular supply, so that "gradually the content of calcium salts becomes greater in the

inner part of the osteon" (1). The model suggests that each view contains an element of the truth: inner lamellae become more highly mineralized because they are close to the blood supply for a longer time during refilling and thereafter.

One of the most important results was the quantitative demonstration that the mineralization of bone cannot be sustained on the basis of simple diffusion as the primary means of transport of mineral ions. The model supports alternative hypotheses that cells or matrix structures augment movement of ions if such transport is concentration gradient-dependent. It is, for example, reasonable to postulate that osteoblasts and osteocytes transport mineral ions through their canalicular processes according to the difference in ionic concentration between two points in this network.

The success of the model in predicting certain basic observations constitutes an obvious strength. At a deeper level, this model, like all mathematical models, is valuable because it enables testing of related hypotheses for internal consistency as a system. There obviously are many limitations to the model. It provides a numerical rather than a closed-form solution, and although care has been taken to ensure that the solutions presented here are not significantly affected by the stability and accuracy problems that can affect such models, future versions also must be carefully checked for such errors. It is two-dimensional in space and one-dimensional in terms of the mineral ions that it considers. It also has not incorporated the hypothesized existence of precursors to hydroxyapatite during calcification.

Although the lack of experimental data defining parametric values is another important limitation of the model, experimentation with the model showed that many of the parameters had to remain within rather narrow ranges to give physiologic results. This provides the basis for two kinds of important hypotheses: hypotheses for experiments designed to determine values for parameters (e.g., does the rate coefficient [k_{cal}] fall within the range suggested by the model?) and hypotheses explaining pathologic conditions (e.g., are certain osteomalacias marked by abnormal values for the rate coefficient [k_{cal}]?). With respect to the latter, it has been shown that aluminum reduces the growth rate of hydroxyapatite crystals (18). The effects of this on the calcification profiles of osteons could be modeled and the resulting calcification profiles compared with microradiographs of osteons affected by aluminum-induced osteomalacia.

It should be noted that some combinations of parametric values caused the model to become quite dynamic. Mineral precipitated at one point was dissolved, moved to another region, and precipitated again. Neuman (13) stressed that there is a continuous exchange of ions back and forth from the solution through the hydration shell to the crystal. The model supports this view that dissolution, exchange, and crystal growth are all part of a continuum, and relatively small changes in local conditions can move the system from one state to another. This, in turn, is consistent with recent theories of calcium homeostasis (17), which postulate the movement of mineral across inactive surfaces, with lining cells and osteocytes controlling equilibrium.

It must be emphasized that this is a preliminary model that should be extended to produce more significant results relevant to current questions about the calcification of bone. Future improvements could include the transport of mineral ions through the osteoblast-canaliculi-osteocyte network, followed by diffusion into the matrix; development of a multiple-ion version based on calcium-phosphate solubility products; and the incorporation of precursor mineral phases.

Acknowledgment: This study was supported by National Aeronautics and Space Administration Grant 2-649. The author is grateful to Brian Bay, Adele Boskey, and Marc Grynpas for their helpful comments.

REFERENCES

1. Amprino R, Engström A: Studies on x ray absorption and diffraction of bone tissue. *Acta Anat* 15:1-22, 1952
2. Anderson HC: Conference introduction and summary (Fifth International Conference on Cell Mediated Calcification and Matrix Vesicles). *Bone Miner* 17:107-112, 1992
3. Bear J, Verruijt A: *Modeling Groundwater Flow and Pollution: With Computer Programs for Sample Cases.* Dordrecht, The Netherlands, D Reidel, 1987
4. Boskey AL, Posner AS: In vitro nucleation of hydroxyapatite by a bone calcium-phospholipid-phosphate complex. *Calcif Tissue Res* 22S:197-201, 1976
5. Boskey AL, Posner AS: Bone structure, composition, and mineralization. *Orthop Clin North Am* 15:597-612, 1984
6. Boskey AL: Hydroxyapatite formation in a dynamic collagen gel system: effects of type I collagen, lipids, and proteoglycans. *J Phys Chem* 93:1628-1633, 1989
7. Bronner F: Dynamics and function of calcium. In: *Mineral Metabolism.* Vol 2, Part A, pp 341-444. Ed by CL Comar and F Bronner. New York, Academic Press, 1964
8. Manson JD, Waters NE: Observations on the rate of maturation of the cat osteon. *J Anat* 99:539-549, 1965
9. Marotti G, Favia A, Zallone AZ: Quantitative analysis on the rate of secondary bone mineralization. *Calcif Tissue Res* 10:67-81, 1972
10. Martin RB, Dannucci GA, Hood SJ: Bone apposition rate differences in osteonal and trabecular bone. *Trans Orthop Res Soc* 12:178, 1987

11. Martin RB, Burr DB: *The Structure, Function, and Adaptation of Compact Bone.* New York, Raven Press, 1989
12. Nancollas GH: In vitro studies of calcium phosphate crystallization. In: *Biomineralization. Chemical and Biochemical Perspectives,* pp 157-187. Ed by S Mann, J Webb, and RJP Williams. New York, VCH, 1989
13. Neuman WF: Chemical dynamics of bone mineral. In: *Bone as a Tissue: Proceedings of a Conference, October 30-31, 1958,* pp 103-117. Ed by K Rodahl, JT Nicholson, and EM Brown Jr. New York, McGraw-Hill, 1960
14. Neuman WF, Neuman MW: Studies of diffusion in calvaria. *Calcif Tissue Int* 33:441-444, 1981
15. Nielsen AE: *Kinetics of Precipitation.* New York, MacMillan, 1964
16. Parfitt AM: The physiologic and clinical significance of bone histomorphometric data. In: *Bone Histomorphometry: Techniques and Interpretation,* pp 143-223. Ed by RR Recker. Boca Raton, CRC Press, 1983
17. Parfitt AM: Bone and plasma calcium homeostasis. *Bone* 8(Suppl 1):S1-S8, 1987
18. Posner AS, Blumenthal NC, Boskey AL: Model of aluminum-induced osteomalacia: inhibition of apatite formation and growth. *Kidney Int Suppl* 18: S17-S19, 1986
19. Simmons DJ, Grynpas MD: Mechanisms of bone formation in vivo. In: *Bone,* pp 193-230. Ed by BK Hall. Caldwell, New Jersey, Telford Press, 1990
20. Thomas WC, Howard JE: Disturbances of calcium metabolism. In: *Mineral Metabolism.* Vol. 2, Part A, pp 445-482. Ed by CL Comar and F Bronner. New York, Academic Press, 1964
21. Weast RC: *CRC Handbook of Chemistry and Physics.* Boca Raton, CRC Press, 1983
22. Weaver JK: The microscopic hardness of bone. *J Bone Joint Surg [Am]* 48:273-288, 1966
23. Widdowson EM, Dickerson JWT: Chemical composition of the body. In: *Mineral Metabolism.* Vol 2, Part A, pp 1-247. Ed by CL Comar and F Bronner. New York, Academic Press, 1964
24. Wuthier RE: The role of phospholipid-calcium-phosphate complexes in biological mineralization. In: *The Role of Calcium in Biological Systems,* pp 41-69. Ed by LJ Anghileri and AM Tuffet-Anghileri. Boca Raton, CRC Press, 1982